Dosage Mutator Genes in *Saccharomyces cerevisiae*: A Novel Mutator Mode-of-Action of the Mph1 DNA Helicase

J. Sidney Ang,*[,1] Supipi Duffy,*[,1] Romulo Segovia,[†] Peter C. Stirling,[†] and Philip Hieter*[,2]
*Michael Smith Laboratories, University of British Columbia, Vancouver, British Columbia V6T 1Z4, Canada and [†]Terry Fox Laboratory, BC Cancer Agency, Vancouver, British Columbia V5Z 1L3, Canada

ABSTRACT Mutations that cause genome instability are considered important predisposing events that contribute to initiation and progression of cancer. Genome instability arises either due to defects in genes that cause an increased mutation rate (mutator phenotype), or defects in genes that cause chromosome instability (CIN). To extend the catalog of genome instability genes, we systematically explored the effects of gene overexpression on mutation rate, using a forward-mutation screen in budding yeast. We screened ~5100 plasmids, each overexpressing a unique single gene, and characterized the five strongest mutators, *MPH1* (mutator phenotype 1), *RRM3*, *UBP12*, *PIF1*, and *DNA2*. We show that, for *MPH1*, the yeast homolog of Fanconi Anemia complementation group M (*FANCM*), the overexpression mutator phenotype is distinct from that of *mph1*Δ. Moreover, while four of our top hits encode DNA helicases, the overexpression of 48 other DNA helicases did not cause a mutator phenotype, suggesting this is not a general property of helicases. For Mph1 overexpression, helicase activity was not required for the mutator phenotype; in contrast Mph1 DEAH-box function was required for hypermutation. Mutagenesis by *MPH1* overexpression was independent of translesion synthesis (TLS), but was suppressed by overexpression of *RAD27*, a conserved flap endonuclease. We propose that binding of DNA flap structures by excess Mph1 may block Rad27 action, creating a mutator phenotype that phenocopies *rad27*Δ. We believe this represents a novel mutator mode-of-action and opens up new prospects to understand how upregulation of DNA repair proteins may contribute to mutagenesis.

KEYWORDS overexpression; mutator; genome-wide; forward mutation; Mph1

CANCER develops by accumulating stepwise genetic mutations in multiple genes that eventually lead to phenotypes such as uncontrolled proliferation and evasion of apoptosis (Vogelstein and Kinzler 2004; Hanahan and Weinberg 2011). Genome instability is an enabling characteristic of cancer, by increasing the likelihood of accumulating mutations in multiple driver genes (Hanahan and Weinberg 2011). Genome destabilizing mutations are thought to occur early during tumor development, reducing the fidelity of DNA transmission and repair, and thereby increasing the likelihood of accumulating multiple gene mutations (Negrini *et al.* 2010; Hanahan and Weinberg 2011).

Genome instability can be classified under two distinct phenotypes: defects that increase mutation rate (mutator phenotype) and defects that increase the rate of aberrations to chromosome number or structure (chromosome instability or CIN). According to the mutator hypothesis, the high rate of genetic changes observed in cancer can be accounted for only by mutations that increase the mutation rate (Loeb 2011). For example, some deficiencies in DNA damage repair components will increase the spontaneous mutation rate, allowing the cells to acquire mutations that may offer a selective advantage and aid in the evolution and progression of tumors (Hanahan and Weinberg 2011).

The budding yeast *Saccharomyces cerevisiae* has been a valuable model system for delineating pathways involved in genome instability, and screens in yeast have identified mutator alleles that increase genome instability (Huang *et al.* 2003; Yuen *et al.* 2007; Stirling *et al.* 2012). A forward

Copyright © 2016 by the Genetics Society of America
doi: 10.1534/genetics.116.192211
Manuscript received June 2, 2016; accepted for publication August 25, 2016; published Early Online August 31, 2016.
Available freely online through the author-supported open access option.
Supplemental material is available online at www.genetics.org/lookup/suppl/doi:10.1534/genetics.116.192211/-/DC1.
[1]These authors contributed equally to this work.
[2]Corresponding author: Michael Smith Laboratories, University of British Columbia, 2185 East Mall, Vancouver, BC V6T 1Z4, Canada. E-mail: hieter@msl.ubc.ca

mutation screen with the nonessential yeast deletion collection identified 33 genes whose null mutations resulted in a mutator phenotype (Huang *et al.* 2003), and 38 essential genes were identified in another screen (Stirling *et al.* 2014). Together, these screens and single gene studies generate a list of 127 yeast mutator alleles (Stirling *et al.* 2014). However, these studies were limited to studying loss-of-function (LOF, nonessential genes) or reduction-of-function (ROF, essential genes) alleles (Huang *et al.* 2003; Stirling *et al.* 2014).

As more cancer genomes are sequenced, it is becoming apparent that somatic copy number amplifications (SCNAs) are one of the most frequent genetic perturbations in cancer (Sanchez-Garcia *et al.* 2014). High recurrence of SCNAs suggests that some may contain cancer drivers (Sanchez-Garcia *et al.* 2014); however, a majority of recurrently amplified regions in tumor genomes ($>$ 70%) do not contain known oncogenes or tumor suppressors (Zack *et al.* 2013). Since amplified regions often encompass multiple genes, identifying drivers remains a challenge (Zack *et al.* 2013), further emphasizing the need for methods to identify functionally relevant genes for tumor biology and progression within SCNAs.

To model potential effects on genome stability of gene amplification and/or overexpression, a genome-wide screen for an overexpression-induced mutator phenotype was conducted. For this purpose, we systematically overexpressed ~85% of the yeast open reading frames using an inducible promoter and assessed increases in the forward mutation rate. We identified 37 genes that we will refer to as dosage mutator (dMutator) genes, the majority of which are involved in DNA replication and DNA damage repair. The top five genes with the highest mutation rate were analyzed further. Overexpressing the DNA helicase *MPH1* (mutator phenotype 1), the yeast homolog of human FANCM, led to the strongest dMutator phenotype, increasing the mutation rate by over 200-fold. Using a series of genetic and functional assays, we show that this phenotype is helicase- and translesion synthesis (TLS)-independent, and DEAH-box function- and *RAD27*-dependent. Thus, the mutator phenotype of *MPH1* overexpression is distinct from that published for *mph1*Δ cells, and suggests a novel gain-of-function mechanism leading to the mutator phenotype. Understanding how gene overexpression can lead to genome instability is a step toward interpreting the roles of amplified and/or overexpressed genome maintenance factors in cancer.

Materials and Methods

Yeast strains and plasmids

Strains and plasmids used are listed in Supplemental Material, Table S2. Strain construction by homologous recombination at chromosomal loci was done using standard methods and confirmed by PCR (Longtine *et al.* 1998). Unless otherwise indicated, standard synthetic media lacking appropriate amino acids for plasmid selection with 2% galactose were used for mutation rate, and other assays. Site-directed mutagenesis of *MPH1* in pDONR221 was performed using a QuikChange kit (Stratagene, La Jolla, CA) following the manufacturer's protocols. All clones were confirmed by sequencing. Genes were shuttled between vectors using Gateway Cloning (Life Technologies). Expression clones were obtained from the Lindquist Gateway Vector collection (Alberti *et al.* 2007).

Dosage mutator screens and confirmations

We used synthetic genetic array (SGA) technology to introduce a wild type *CAN1* gene into the overexpression array (Tong *et al.* 2001). A query strain containing *avt2*Δ::KANMX was crossed to the yeast full-length expression ready (FLEX) array, each containing a plasmid with a single gene under the control of the *GAL1* promoter (Douglas *et al.* 2012). The *AVT2* gene is immediately adjacent to the *CAN1* gene; thus, *avt2*Δ::KANMX provides a linked marker for selection of spores carrying the wild-type *CAN1* locus. Following replica pinning steps, we generated an output array containing the *avt2*Δ::KANMX and the individual overexpression plasmids.

Cells were taken from the haploid selection plates and streaked to single colonies on haploid selection medium (SD-U-L-K+G418+Thialysine) and grown for 2 days at 30°. Two induction steps were used to maximize the overexpression of genes from the plasmids. For the first induction, individual colonies were selected from the haploid selection plates and patched in duplicate onto medium containing galactose (SG-U-L-K+G418+Thialysine) and grown for 2 days at 30°. Subsequently, for the second induction, cells from these patches were patched again into 1 cm $\times$ 1 cm patches on galactose-containing medium (SG-URA+G418). Patches were grown for 2 days at 30° and cells were replica plated onto CAN^R selection plates (SD-R+ 50 μg/ml Canavanine). Plates were scored manually by counting colonies after incubating at 30° for 2–3 days.

Direct transformations were used to validate our hits from the genome-wide mutator screen. Plasmids from the FLEX array were verified by DNA sequencing, and then transformed directly into a wild-type BY4741 strain, and single colonies were patched twice, in quadruplicate, onto galactose containing media (SG-U) for induction. Patches were then replica plated onto canavanine plates (SD-R+CAN) and scored as above.

Fluctuation analyses

Mutation rates per cell division were adapted from a previously described assay (Lang and Murray 2008). Briefly, four independent transformants from each strain were grown to saturation in synthetic complete medium lacking uracil and supplemented with galactose (SG-URA). Each saturated culture was diluted 1:10,000 into 24 wells of SG-URA and grown for 2 days at 30°. Six random wells for each gene being tested were pooled and used to determine an average cell count using a TC20 cell counter (Bio-Rad, Hercules, CA). The remaining 18 wells were plated

onto plates containing medium supplemented with glucose and 50 μg/ml canavanine but lacking arginine (SD-ARG+Canavanine). Plates were incubated at 30° for 2–3 days. Plates were scored for the frequency of Can^R colonies. Rates per generation were determined using the Ma-Sandri-Sarkar maximum-likelihood method calculated by the FALCOR program (Hall *et al.* 2009).

Serial spot dilutions

Strains were grown to saturation at 30° in synthetic complete medium lacking uracil. Cultures were diluted to an OD_{600} of 1 and plated in 10-fold serial dilutions onto plates supplemented with galactose and containing the DNA-damaging agents (DDAs) methyl methanesulfonate (MMS), camptothecin (CPT), and hydroxyurea (HU) at concentrations of 0.01%, 25 μg/ml, and 50 mM, respectively.

Growth curve and analysis

Strains were grown to saturation at 30° in synthetic complete medium lacking uracil. Two microliters of the saturated culture was diluted into 200 μl of the appropriate medium containing galactose and DDAs (at concentrations specified above). OD_{600} measurements were measured by a Tecan M200 plate reader at 30 min intervals for 72 hr at 30°. Area-under-the-curve analysis was performed as previously described (Hamza *et al.* 2015).

Chromosome region specific effects

Strains containing *URA3* located at different locations along chromosome VI (Lang and Murray 2008) were transformed with *MPH1* overexpression plasmid marked with *HIS3*. Transformants were patched in quadruplicate onto SG-URA-HIS medium and incubated at 30° for 2 days to induce overexpression. Patches were replica-plated onto SD-URA+5-FOA and incubated for 2 days.

Dependence on TLS pathway

TLS mutants, *rev1Δ*, *rev3Δ* and *rad30Δ*, from the yeast deletion collection (Winzeler *et al.* 1999) were transformed with the *MPH1* overexpression plasmid and were patched onto SG-URA plates in triplicate. After 2 days incubation at 30°, patches were replica plated onto SD-R+canavanine and incubated for 2–3 days at 30°.

Data availability

Strains are available upon request. Table S2 contains all strains and plasmids used in this study.

Results

Systematic identification of dmutator genes using overexpression

To uncover genes whose overexpression results in an increased mutation rate, we performed a genome-wide screen in yeast. We screened an arrayed collection of yeast strains overexpressing ~5100 genes under the control of a galactose-inducible promoter for increased forward mutagenesis of the *CAN1* marker (Hoffmann 1985; Douglas *et al.* 2012). Using SGA technology (Tong *et al.* 2001), we introduced a wild-type copy of the *CAN1* gene into each of the yeast strains in the overexpression array, and screened for canavanine resistant (CAN^R) mutants in triplicate patches (Figure 1A). After screening ~5100 genes and confirming the primary hits with direct tests using sequence verified plasmids (see *Materials and Methods*), we generated a list of 37 dMutator genes whose overexpression increased the frequency of CAN^R mutants as compared to a vector alone control (Table 1). Approximately half of the dmutator genes (18/37) function in biological pathways such as DNA damage repair, DNA replication, or transcription, processes well known to influence genome instability (Saccharomyces Genome Database). For 12 of the genes, overexpression also increases chromosome instability (Duffy *et al.* 2016), highlighting the established considerable overlap between the mutator and chromosome instability phenotypes (Stirling *et al.* 2011).

Prior to this work, *MLH1* was the only previously known dmutator gene (Shcherbakova and Kunkel 1999). Since it was not in the overexpression array, we tested directly the overexpression of *MLH1* in our assay. Indeed, overexpression of *MLH1* induced a dMutator phenotype under a galactose-inducible promoter (Figure 1B).

Determining mutation rate by fluctuation analysis

To determine the mutation rate of the dMutator genes, we used fluctuation analysis (Luria and Delbrück 1943; Lang and Murray 2008) and selected the top five dMutator genes, *MPH1*, *UBP12*, *PIF1*, *RRM3*, and *DNA2*, for further analysis. Overexpressing any one of these genes increased the mutation rate by at least 3-fold compared to a vector alone control (Figure 1C). Since four of these genes encode helicase activity, we reasoned that something common to ectopic helicase activity could be driving mutagenesis. To assess this possibility, we directly retested 48 DNA helicases using the *CAN1* mutator assay to determine whether they had been false negatives in the screen (Table S1). However, none of the additional helicases tested conferred a mutator phenotype when overexpressed, suggesting both that helicase activity alone is not a predictor of the dMutator phenotype and that the false negative rate of our assay was probably very low. Of the five identified dMutator genes, *MPH1*, a 3′–5′ DNA helicase and a sequence homolog of the human FANCM, resulted in a >200-fold increase in mutation rate (Figure 1C). While *MPH1* deletion also results in a mutator phenotype (Entian *et al.* 1999), the mutation rates are dramatically different (Table 2).

Dosage mutator genes affect DNA metabolism

It is clear how the LOF or the ROF of a cellular protein may lead to a phenotype such as an increased mutator rate; however, it is not as clear how overexpression may affect this phenotype. Therefore, we wanted to further explore the mechanism behind the mutator phenotype for our top five dMutator genes. LOF alleles of two of the top five dMutator genes,

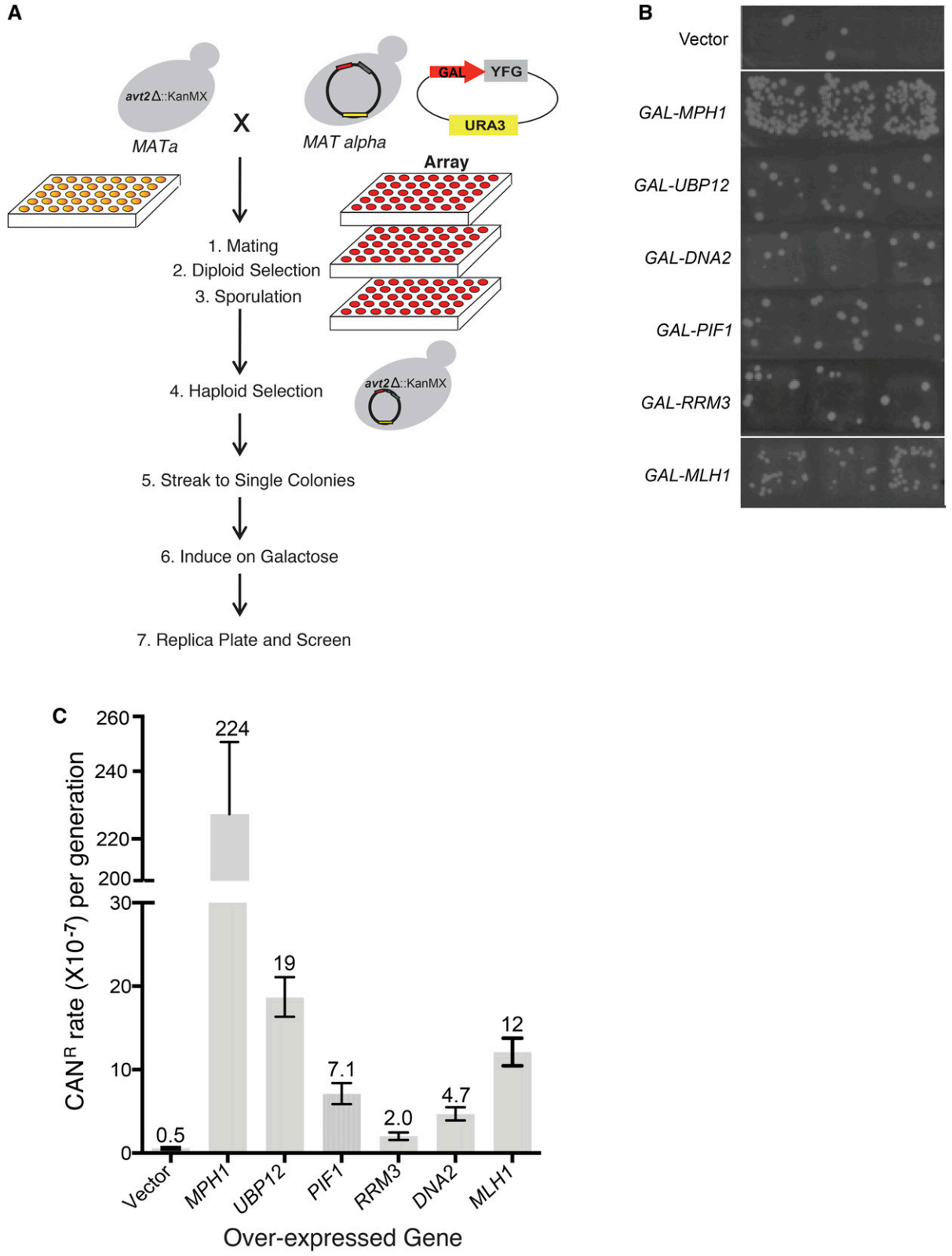

Figure 1 Dosage mutator (dMutator) screen workflow. (A) The overexpression array was mated to a query strain with *avt2*Δ::KANMX, which is immediately adjacent to the wild-type *CAN1* gene using SGA. Following replica pinning steps, a haploid output array was generated where each strain contained both a unique gene overexpression plasmid and the wild type *CAN1* gene. Haploid cells were streaked onto selective medium to obtain single colonies, and overexpression was induced by plating on medium containing 2% galactose. Cells were replica plated onto medium containing canavanine 48 hr postinduction to assess the mutator phenotype. (B) Top dMutator genes from our screen overexpressing the indicated genes with the vector alone control for comparison. *MLH1* was tested as a positive control. Each gene was tested in triplicate and each patch represents an independent

Table 1 Validated dMutator genes identified on solid media

ORF	Gene
YBR234C	ARC40
YER177W	BMH1
YNL042W	BOP3
YMR078C	CTF18
YHR164C	DNA2
YKL204W	EAP1
YDR434W	GPI17
YDR378C	LSM6
YLR274W	MCM5
YNL173C	MDG1
YIR002C	MPH1
YGR220C	MRPL9
YKR087C	OMA1
YPR162C	ORC4
YML061C	PIF1
YLR196W	PWP1
YML032C	RAD52
YGL163C	RAD54
YDR004W	RAD57
YBR087W	RFC5
YGL044C	RNA15
YBR181C	RPS6B
YHR031C	RRM3
YBR130C	SHE3
YFL008W	SMC1
YGL207W	SPT16
YML010W	SPT5
YHR041C	SRB2
YGL097W	SRM1
YLR005W	SSL1
YCR042C	TAF2
YOL006C	TOP1
YJL197W	UBP12
YIL017C	VID28
YDR248C	YDR248C
YGR126W	YGR126W
YHR122W	YHR122W
YMR167W	MLH1

PIF1 and *MPH1*, also increases the mutation rate (Entian *et al.* 1999; Huang *et al.* 2003), suggesting that, in these instances, overexpression may phenocopy LOF. To test this possibility, we chose to examine whether the phenotypic concurrence between overexpression and LOF will hold true for additional phenotypes.

Defective DNA repair is a well-established mechanism that leads to a mutator phenotype (Jackson and Bartek 2009), which often renders cells hypersensitive to DDAs. Thus, sensitivity to DDAs was an independent assay that could be utilized to compare directly the overexpression and LOF alleles of the dMutator genes. We tested the sensitivity of the top five dMutator genes to three DDAs—methyl methanesulfonate (MMS), hydroxyurea (HU) and camptothecin (CPT)—along with LOF alleles for *mph1Δ*, *ubp12Δ*, and *rrm3Δ* (Figure 2, A and B). Direct comparison data were not collected for *DNA2* as it is an essential gene and *pif1Δ* does not grow on galactose (Figure 2A). Strains were determined to be "sensitive" or "not-sensitive" to DDAs based on relative percent fitness as measured by area-under-the-curve in liquid growth assays ($P < 0.05$) (Figure 2C). Overexpressing *MPH1* sensitized cells to all three DDAs, whereas overexpressing *UBP12* and *RRM3* increased sensitivity only to MMS and HU, or MMS and CPT, respectively (Figure 2C). Thus, the sensitivity profiles for *MPH1*, *RRM3*, and *UBP12* overexpression were distinct from the sensitivity profile of the corresponding deletes, suggesting a different mode of action for overexpression-induced mutator phenotype.

Table 2 Mutation rates of *MPH1* overexpression and deletion

	Mutation Rate (10^{-7})	95% C.I. Upper Bound (10^{-7})	95% C.I. Lower Bound (10^{-7})
GAL-MPH1	224	251	199
mph1Δ	11.1	12.6	9.83

We further tested the dMutator genes for the presence of increased DNA damage using Rad52 as a proxy. Rad52 is essential for homologous recombination and forms foci in response to double strand breaks (DSBs) leading to recombination events (Lisby *et al.* 2001; Symington 2002). The overexpression of one dMutator gene, *RRM3*, increased Rad52-foci (Figure 2, D and E). *RRM3* deletion also increases Rad52 foci (Alvaro *et al.* 2007); therefore, these data suggest that cells that either lack or overexpress *RRM3* may induce dependence on DNA repair through homologous recombination. However, this is the only phenotype for which we see concurrence between *RRM3* overexpression and deletion, as the DDA sensitivity profile for *RRM3* overexpression is distinct from the deletion mutant, and *rrm3Δ* does not induce a mutator phenotype. Together our analysis implies that the dMutator phenotype is not generally due to a LOF upon overexpression and must relate to an inappropriate gain-of-function.

The dMutator phenotype of MPH1 is partially dependent on the TLS pathway

We wanted to further understand the mechanisms behind the mutator phenotype of *MPH1*, as it was the strongest dMutator gene identified in our screen. The *MPH1* deletion also results in a mutator phenotype (Entian *et al.* 1999); however, the mechanism behind the mutator phenotype may be different since the mutation rates are dramatically different between *mph1*Δ and *MPH1* overexpression (Table 2), and because the DDA sensitivity profiles for *MPH1* deletion and the overexpressor are distinct (Figure 2C).

The mutator phenotype of the *mph1*Δ mutant is dependent on TLS (Scheller *et al.* 2000; Schurer 2004). TLS allows bypassing of DNA lesions so replication can resume, and

transformant. For a complete list see Table 1. (C) Overexpression of *MPH1*, *UBP12*, *PIF1*, *RRM3*, and *DNA2* resulted in an increased mutation rate > 2-fold higher compared to a vector alone control. Mutation rates were quantified using fluctuation analysis. Error bars represent 95% confidence intervals with the average mutation rate shown above each bar.

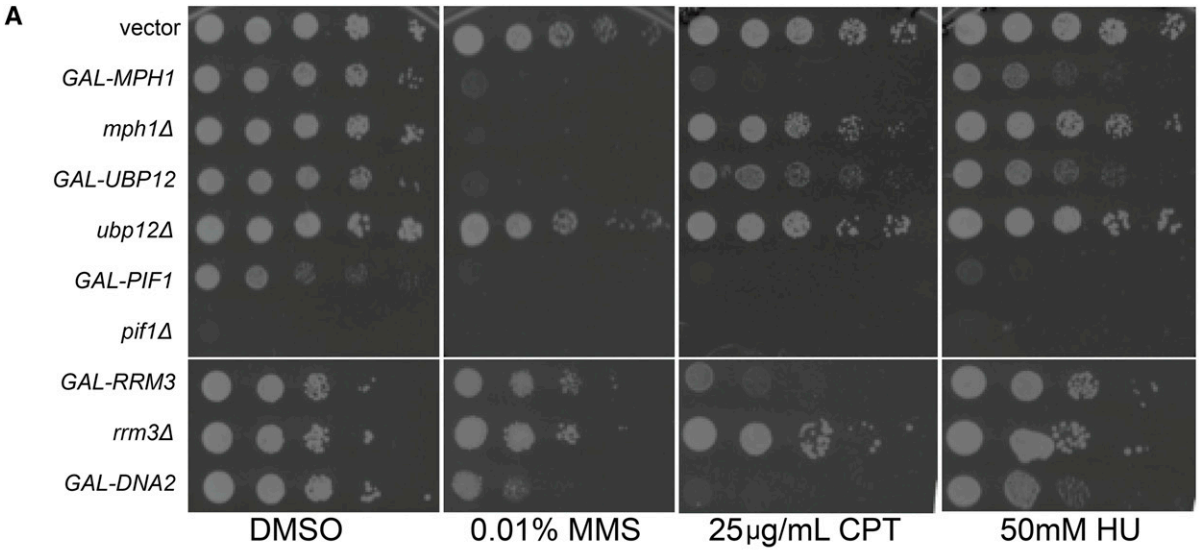

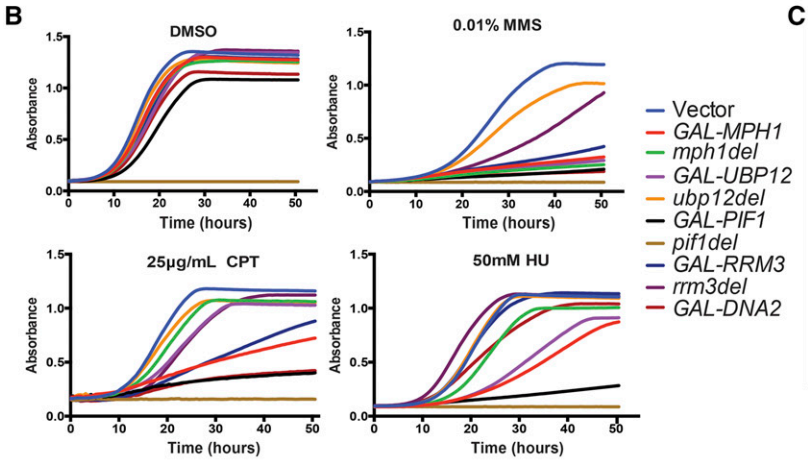

C

	MMS	CPT	HU
GAL-MPH1	32	53	51
mph1Δ	27	88	83
GAL-UBP12	30	81	58
ubp12Δ	81	91	100
GAL-PIF1	33	36	25
pif1Δ	13	19	12
GAL-RRM3	36	55	101
rrm3Δ	56	81	108
GAL-DNA2	39	36	86

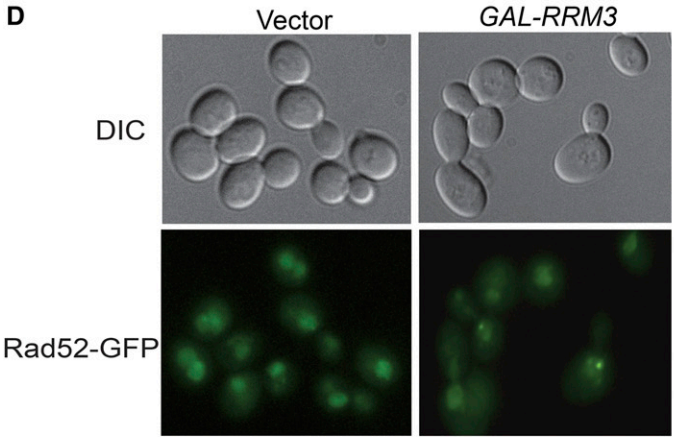

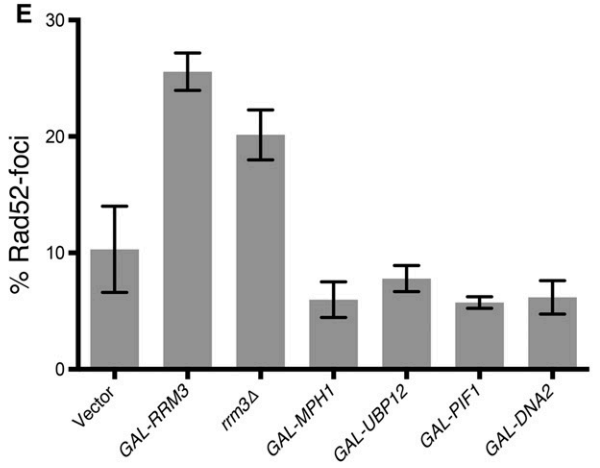

Figure 2 Overexpression of dMutator genes induces sensitivity to DDAs. (A) Serial spot dilutions of dMutator genes and respective deletion mutants on galactose, in the presence of the DDAs indicated. Deletion mutants were transformed with empty vector to enable tests on comparable growth medium. (B) Liquid growth curves of the dMutator genes and respective deletion mutants in galactose and in the presence of the indicated DDAs. (C) DDA sensitivities of dmutator genes and corresponding deletion mutants based on the liquid growth assays. Numbers represent relative percent fitness as measured by area-under-the-curve for each strain in triplicate. Red shading represents sensitive strains, and green shading represents strains that are not sensitive to drugs ($P < 0.05$). (D) Sample images of a reporter strain with Rad52-GFP was transformed with a plasmid overexpressing *RRM3* or a vector alone control. (E) Quantified data for Rad52-foci in strains overexpressing dMutator genes and a *rrm3*Δ. Data summarizes three independent experiments where > 100 cells were counted for each replicate.

involves several DNA polymerases that include Rev3 (DNA polymerase zeta), Rad30 (DNA polymerase eta), and Rev1 (deoxycytidyl transferase) (Johnson 1999; Friedberg 2002). A large portion of spontaneous mutations in the *mph1*Δ mutants arises by Rev3-mediated mutagenic bypass of DNA lesions using the error-prone TLS pathway (Scheller *et al.* 2000). Therefore, we tested if the mutator phenotype of *MPH1* overexpression also relied on the TLS pathway. We transformed deletion mutants of the TLS polymerases *REV1*, *REV3*, and *RAD30* with a plasmid overexpressing *MPH1* and assayed for a mutator phenotype at *CAN1*. We did not observe a reduction in the frequency of CAN^R mutants in the individual TLS mutants (Figure 3A). We next generated double and triple mutants of TLS polymerases and quantified the mutation rate of *MPH1* overexpression in these mutants. Removal of *REV3* together with *REV1* or *RAD30* partially reduced the frequency of CAN^R mutants, and the simultaneous removal of all three TLS polymerases also reduced this frequency, although not more than the double mutants (Figure 3A). Thus, similar to the *mph1*Δ mutants, the mutagenesis induced by overexpression of *MPH1* relies on Rev3-mediation mutagenic bypass; however, unlike the mutator phenotype of *mph1*Δ, mutations caused by *MPH1* overexpression are only partially dependent on the TLS pathway.

The dMutator phenotype of Mph1 depends on the DEAH-box but not on catalytic activity

To further examine the dMutator phenotype, we next turned to the catalytic activities of *MPH1*. Mph1 possesses three conserved motifs: a DEAH-box (Scheller *et al.* 2000), an ATPase domain (Prakash *et al.* 2005), and a helicase domain (Kang *et al.* 2012). To determine whether catalytic activity (helicase and ATPase) and DEAH-box functions were necessary for the dMutator phenotype, we generated five point mutations that have been described previously. It has been shown that all these mutant proteins are expressed at similar levels and localize to the nucleus (Scheller *et al.* 2000). These include an ATPase mutant (K113Q), a helicase mutant (Q603D), and three DEAH-box mutants (D209N, E210Q, and H212D) (Banerjee *et al.* 2008). All of these mutations are predicted to impair the helicase activity, and one, D209N, to lack both ATPase and helicase activity but was proficient in DNA binding *in vitro* (Prakash *et al.* 2009).

The overexpression of all five single point mutants resulted in an overexpression mutator phenotype that was similar to that seen when wild-type *MPH1* was overexpressed (Figure 3B). Therefore, similar to observations made with *MPH1* overexpression-induced gross chromosomal rearrangement (Banerjee *et al.* 2008), the mutator phenotype of *MPH1* overexpression does not appear to be due to the hyperactivation of the helicase or ATPase activities. However, while single DEAH point mutations had no effect, overexpressing double DEAH-box mutants (D209N, E210Q), (D209N, H212D), and (E210Q, H212D), or the triple DEAH-box mutant (D209N, E210Q, and H212D) with impaired Mg^{+2} binding, ATP hydrolysis and/or NTP-dependent conformational change, and possibly protein stability or interaction defects (Scheller *et al.* 2000), lowered the mutation rate tremendously to near normal levels as compared to *MPH1* (Figure 3B).

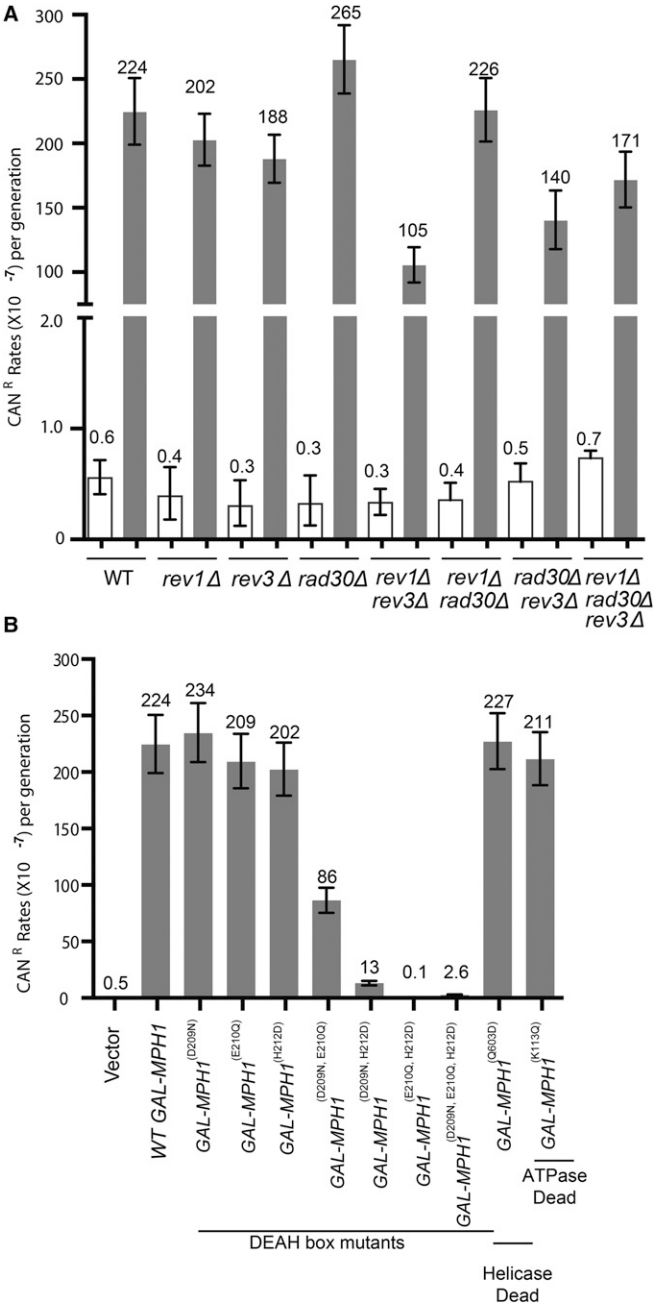

Figure 3 dMutator phenotypes of *MPH1*. (A) Mutation rates for overexpression of *MPH1* in *rev1*Δ, *rev3*Δ, or *rad30*Δ mutants, along with the vector alone control, as determined by fluctuation analysis. Error bars represent 95% confidence intervals with the average mutation rate shown above each bar. Empty vector (white bars), MPH1 expressing (gray bars). (B) Mutation rates when *MPH1* catalytic mutants, ATPase mutant (K113Q), a helicase mutant (Q603D), individual DEAH-box mutants (D209N, E210Q, and H212D), combined double DEAH-box mutants, and the triple DEAH-box mutants, were overexpressed and assessed using fluctuation analysis. Error bars represent 95% confidence intervals with the average mutation rate shown above each bar.

Mutations caused by MPH1 overexpression are localized to the telomeres

Overexpression of *MPH1* also leads to the accumulation of single-stranded DNA (ssDNA) at telomeres (Luke-Glaser and Luke 2012). ssDNA can be more prone to damage since the nucleotides are more exposed to reactive species. Given that *CAN1* was at the distal region of chromosome V, it seemed possible that the increased mutation rate at *CAN1* is due to the presence of ssDNA. To determine whether gene position on the chromosome affected the mutation rate, we used strains in which *URA3* was integrated at different locations on chromosome III (Figure 4A) (Lang and Murray 2008). Overexpressing *MPH1* exhibited a mutator phenotype only when *URA3* was located in the most telomeric regions (Figure 4B), while this phenotype is more generalized for other dMutator genes such as *UBP12* and *DNA2* (Figure S1, A and B).

The mutator phenotype of Mph1 is dependent on levels of Rad27 and Dna2

Since the dMutator activity of Mph1 depends on its DEAH box but not its specific catalytic activities, we reasoned that the mechanism may rely on competition for DNA binding with another DNA-binding protein. One ideal candidate is the flap endonuclease, Rad27. Both Mph1 and Rad27 are known to bind DNA flap structures and work in Okazaki fragment processing (Kang *et al.* 2009, 2012). One possibility is that when Mph1 is overexpressed it outcompetes the action of Rad27 from these structures, mimicking a *RAD27* deletion. Alternatively, Mph1 has been shown to stimulate Rad27 *in vitro*, and this hyperactivity could be mutagenic. Also, consistent with coordinated action of Mph1 and Rad27 is that deletion of *RAD27* has been reported to increase instability and ssDNA at telomeres (Parenteau and Wellinger 1999), and to cause a strong mutator phenotype (Tishkoff *et al.* 1997). Accordingly, while overexpressing *RAD27* alone had no effect on the mutator phenotype, overexpressing *RAD27* lowered the mutator phenotype caused by *MPH1* overexpression (both qualitatively and quantitatively by fluctuation analysis) as compared to overexpressing *MPH1* alone (Figure 4, C and D). Additionally, *rad27*Δ had a strong mutator phenotype that was not further enhanced by overexpression of *MPH1* (Figure 4D). This epistatic relationship shows that *MPH1* overexpression and *RAD27* deletion work in the same mutagenesis pathway. Rad27 and Dna2 work coordinately in Okazaki fragment processing (Bae *et al.* 2001), and we also observed that overexpression of *DNA2* reduced significantly the dMutator effect of *MPH1*, suggesting that lagging strand replication may be a target for mutagenesis by the *MPH1* dMutator activity (Figure 4D).

Given that the mutator phenotype of *MPH1* overexpression phenocopies the LOF mutation of *RAD27*, we tested whether this concordance was limited to the mutator phenotype or holds true for other phenotypes such as negative genetic interactions. Negative genetic interactions such as synthetic lethality takes place when the observed fitness defect of a double mutant is significantly less than that of the expected fitness based on the fitness of the two single mutants (Mani *et al.* 2008). Overexpression of *MPH1* caused synthetic dosage lethality in strains lacking *MUS81*, *ELG1*, and *MMS1*, but had no phenotype in *RAD1*, *CHL1*, and *EXO1* deletions (Figure 4E). This suggests that the mutator phenotype of *MPH1* overexpression is only partially redundant with loss of *rad27*Δ. Interestingly, among those tested, mutations with specific functions in handling DNA replication stress (*i.e.*, *mus81*Δ, *elg1*Δ, and *mms1*Δ) appear to be most negatively affected by *MPH1* overexpression, possibly suggesting that the replication role of Rad27 is the relevant activity.

To further establish that *MPH1* overexpression increases mutation rate by either outcompeting or squelching its functional partners or those of Rad27, we chose to examine the effect of removing, *SGS1*, *MUS81*, and *SRS2* on the dMutator phenotype. *SGS1* encodes another DNA helicase, which functions in parallel with Mph1 to regulate the choice of homologous recombination pathway to be used (Jain *et al.* 2016), the endonuclease Mus81 and the Srs2 helicase also influence repair pathway choice and recombination intermediate processing (Mazón and Symington 2013; Mitchel *et al.* 2013). Deletion of *SGS1* or *MUS81* led to small but significant decreases in the dMutator phenotype of *MPH1* overexpression (Figure 4F), while deletion of *SRS2* led to a $>$ 5-fold decrease in mutation rate (Figure 4F).

Discussion

A genome-wide screen for genes that, when overexpressed, increased the mutation rate, identified 37 dMutator genes in yeast. The majority of these genes belong to biological processes, such as DNA repair, previously known to impact mutation rate, and ~30% of the dMutator genes also cause chromosome instability as seen previously for LOF and ROF mutations (Stirling *et al.* 2012). Incorporating the data from our screen with published data, a total of 210 genes are implicated in increasing the mutator phenotype in yeast (Huang *et al.* 2003; Stirling *et al.* 2012).

The five strongest dMutator genes, *MPH1*, *UBP12*, *PIF1*, *RRM3*, and *DNA2*, had mutation rates at least two times greater than wild type (Figure 1C). Since four of these genes possess helicase activity, we tested directly whether ectopic helicase activity is responsible for the dMutator phenotype by overexpressing a panel of other DNA helicases, and found that helicase activity itself did not predict the dMutator phenotype. We further characterized the top five dMutator genes by examining their sensitivities to DDAs, and their effects on DNA integrity. Cells overexpressing any one of the five dMutator genes were sensitive to DDAs, implicating defective DNA repair as one possible mechanism for the dMutator phenotype (Figure 2, A and B). However, overexpression of only one gene, Rrm3, induced higher than wild type levels of Rad52 foci (Figure 2E). Consequently, the dMutator phenotype of Rrm3 may be due to both increased DNA damage and defective DNA repair. When the DDA sensitivity profiles of

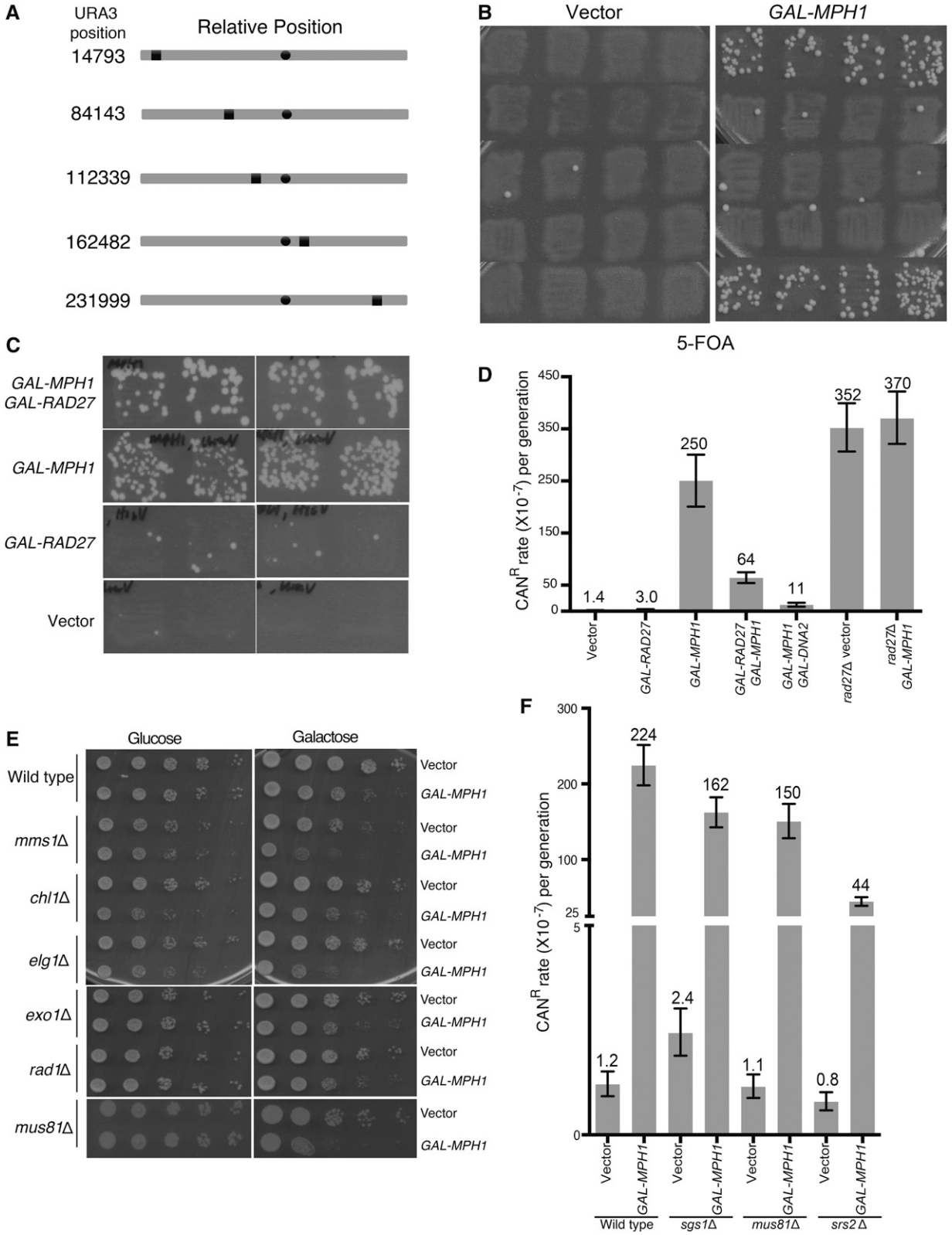

Figure 4 *MPH1* dMutator phenotype is position-dependent and is epistatic to Rad27. (A) Schematic of absolute and relative positions of *URA3* position along chromosome III. The black circle represents the centromere, and the black boxes represent the location of the *URA3* gene relative to the centromere and the telomere. Numbers beside each schematic denotes the absolute position of *URA3* on the chromosome. (B) Strains containing *URA3* at positions indicated in (A) with a vector alone control or with the overexpression of *MPH1*. Each strain was assayed with four independent transformants. (C) The mutator phenotype of strains overexpressing *RAD27* (URA marked), *MPH1* (HIS marked), or both plasmids together along with the vector alone controls. (D) Mutation rates of strains overexpressing *RAD27*, *MPH1*, *RAD27*, and *MPH1*, as well as a *rad27Δ* strain overexpressing

MPH1, *RRM3*, and *UBP12* were compared directly to the corresponding LOF alleles there was no concurrence between the profiles, implying different mechanisms of action (Figure 2C). In the case of *MPH1*, whose LOF allele also induces a mutator phenotype, the unique sensitivity profile to DDAs suggests that overexpression does not mimic deletion in this case (Veitia 2005). Taken together, these data suggest that dMutators are relatively rare, and, while they function in the same pathways as canonical mutators (such as DNA repair), overexpression causes mutations by different mechanisms as compared to LOF or ROF.

The differences in mechanism of action between overexpression and deletion were particularly pronounced for *MPH1*. *MPH1* overexpression caused sensitivity to MMS, CPT, and HU, whereas *MPH1* deletion caused sensitivity only to MMS (Figure 2, A and B). *MPH1* overexpression also caused a higher mutation rate than the *MPH1* deletion and, furthermore, the mutator phenotype caused by *MPH1* overexpression was at least partially independent of TLS polymerases (Figure 3A and Table 2). We also showed that the *MPH1* dMutator phenotype was independent of the helicase and ATPase activities of Mph1, but was abrogated by simultaneously mutating either two or three residues in the DEAH domain (Figure 3B). These DEAH mutations may also abolish binding to Mg^{+2}, ATP hydrolysis, and/or the NTP-dependent conformational change, suggesting to us that proper DEAH-box function is the essential feature of its dMutator mechanism. Alternatively, the result of the multiple DEAH mutants may be impaired protein- or DNA-binding interfaces, which could arise due to conformational changes in the protein or because the protein has become unstable. Either way our analysis implicates noncatalytic functions of Mph1 in inducing *CAN1* hypermutation.

RAD27 deletion causes a mutation rate comparable to *MPH1* overexpression (Huang *et al.* 2003), and an increase in telomeric ssDNA (Parenteau and Wellinger 1999), as has been seen previously with *MPH1* overexpression (Luke-Glaser and Luke 2012) (Figure 4B). Prompted by these similarities, we tested for genetic interactions between *MPH1* and *RAD27*. Deletion of *RAD27* was epistatic to *MPH1* overexpression with respect to mutation rate (Figure 4D). This suggested that hypermutation in Mph1 overexpressing cells is mediated by impairing the Rad27 pathway. Consistent with this interpretation, overexpressing *RAD27* or *DNA2* [which works in parallel with Rad27 in Okazaki fragment processing (Bae *et al.* 2001)], together with *MPH1* strongly reduced the mutation rate compared to *MPH1* alone (Figure 4C). These data suggest that the relative stoichiometry of Mph1, Rad27, and Dna2 is critical to prevent mutations.

Several lines of evidence support defective replication as a mechanism for the dMutator phenotype of *MPH1*: (1) *MPH1* overexpression recapitulated the genetic interactions between *rad27*Δ and DNA replication fork protection factors such as *mms1*Δ, *mus81*Δ, and *elg1*Δ (Figure 4E); (2) the position specific mutation rate increases we saw for *URA3* at subtelomeric loci in Chr VI (Figure 4B) occur in late replicating regions of the chromosome (Lang and Murray 2011); and (3) removal of *SRS2* strongly suppressed the dMutator phenotype of *MPH1* overexpression (Figure 4F). Srs2 has a previously identified antimutator activity in deletions of *MMS2*, a ubiquitin-conjugating enzyme required for postreplicative repair (Broomfield and Xiao 2002). In addition, defects in Okazaki fragment processing caused by loss of *RAD27* have been shown to activate postreplicative repair via the exposure of ssDNA (Parenteau and Wellinger 1999). Indeed, as with our data on *MPH1* overexpression, these authors showed that mutation rates in *rad27*Δ cells were suppressed only partially by deletion of *REV3* (Becker *et al.* 2015).

Together, these data lead us to propose a model where high levels of Mph1 lead to dysregulation of Okazaki fragment processing (Kang *et al.* 2009, 2012), signaling via Srs2 to the postreplicative repair and to damage-tolerance/TLS pathways, which together increase the frequency of mutations. This is particularly pronounced in late-replicating and/or subtelomeric regions, where both *MPH1* overexpression or *rad27*Δ are known to enhance the exposure of ssDNA. While the enzymatic activity of Mph1 is not required for the dMutator effect, increasing the concentration of Rad27 or Dna2 in the cell can revert the dMutator phenotype. Therefore, we favor the view that competition for DNA flap binding by excess Mph1 may impair normal flap processing sufficiently to trigger mutations.

The human *MPH1* homolog *FANCM* is a breast cancer susceptibility gene that is characterized by missense or nonsense somatic mutations in cancer cells (Kiiski *et al.* 2014; Peterlongo *et al.* 2015). There are also examples of *FANCM* overexpression in cancer that are of unknown significance (Cerami *et al.* 2012; Gao *et al.* 2013). Our study shows that the overexpression of DNA repair proteins, specifically Mph1, can cause imbalances in DNA transactions through competition to drive mutagenesis. Further analysis of the effects of gene overexpression on genome instability should reveal new mechanisms by which protein imbalances affect genome maintenance.

Acknowledgments

We thank Brenda Andrews for the FLEX overexpression collection and Nigel O'Neil for helpful discussions and advice. This work was funded by grants from the Canadian Institute of Health Research (CIHR) (MOP 38096) and the National Institutes of Health (RO-1CA158162) to P.H. and a

MPH1 or a vector alone control assayed using fluctuation analysis. Error bars represent 95% confidence intervals, with the average mutation rate shown above each bar. (E) Synthetic dosage lethal interactions with *MPH1* for mutations that are synthetic lethal with a *RAD27*-null mutant. (F) Mutation rates for strains lacking *SGS1*, *MUS81*, and *SRS2* overexpressing *MPH1* or a vector alone control assayed using fluctuation analysis. Error bars represent 95% confidence intervals with the average mutation rate shown above each bar.

Canadian Institute for Advance Research Global Fellowship and a CIHR Banting Fellowship to S.D. P.C.S. is a CIHR New Investigator and Michael Smith Foundation for Health Research scholar, and acknowledges funds from CIHR (MOP-136982) and that this research is funded by the Canadian Cancer Society (grant 703263). P.H. is a Senior Fellow in the Genetic Networks program at the Canadian Institute for Advanced Research. The authors declare no conflict of interest.

Literature Cited

Alberti, S., A. D. Gitler, and S. Lindquist, 2007 A suite of gateway cloning vectors for high-throughput genetic analysis in *Saccharomyces cerevisiae*. Yeast 24(10): 913–919.

Alvaro, D., M. Lisby, and R. Rothstein, 2007 Genome-wide analysis of Rad52 Foci reveals diverse mechanisms impacting recombination. PLoS Genet. 3(12): e228.

Bae, S. H., K. H. Bae, J. A. Kim, and Y. S. Seo, 2001 RPA governs endonuclease switching during processing of Okazaki fragments in eukaryotes. Nature 412(6845): 456–461.

Banerjee, S., S. Smith, J.-H. Oum, H.-J. Liaw, J.-Y. Hwang *et al.*, 2008 Mph1p promotes gross chromosomal rearrangement through partial inhibition of homologous recombination. J. Cell Biol. 181(7): 1083–1093.

Becker, J. R., C. Pons, H. D. Nguyen, M. Costanzo, C. Boone *et al.*, 2015 Genetic interactions implicating postreplicative repair in Okazaki fragment processing. PLoS Genet. 11(11): e1005659.

Broomfield, S., and W. Xiao, 2002 Suppression of genetic defects within the RAD6 pathway by srs2 is specific for error-free postreplication repair but not for damage-induced mutagenesis. Nucleic Acids Res. 30(3): 732–739.

Cerami, E., J. Gao, U. Dogrusoz, B. E. Gross, S. O. Sumer *et al.*, 2012 The cBio cancer genomics portal: an open platform for exploring multidimensional cancer genomics data. Cancer Discov. 2(5): 401–404.

Douglas, A. C., A. M. Smith, S. Sharifpoor, Z. Yan, T. Durbic *et al.*, 2012 Functional analysis with a barcoder yeast gene overexpression system. G3 (Bethesda) 2(10): 1279–1289.

Duffy, S., H. K. Fam, Y. K. Wang, E. B. Styles, J. H. Jim *et al.*, 2016 Overexpression screens identify conserved dosage chromosome instability genes in yeast and human cancer. Proc Natl Acad Sci USA 113(36): 9967–9976.

Entian, K. D., T. Schuster, J. H. Hegemann, D. Becher, H. Feldmann *et al.*, 1999 Functional analysis of 150 deletion mutants in *Saccharomyces cerevisiae* by a systematic approach. Molecular & General Genetics: MGG 262(4–5): 683–702.

Friedberg, E. C., 2002 Specialized DNA polymerases, cellular survival, and the genesis of mutations. Science 296(5573): 1627–1630.

Gao, J., B. A. Aksoy, U. Dogrusoz, G. Dresdner, B. Gross *et al.*, 2013 Integrative analysis of complex cancer genomics and clinical profiles using the cBioPortal. Sci. Signal. 6(269): pl1.

Hall, B. M., C.-X. Ma, P. Liang, and K. K. Singh, 2009 Fluctuation analysis calculatOR: a web tool for the determination of mutation rate using Luria-Delbruck fluctuation analysis. Bioinformatics 25(12): 1564–1565.

Hamza, A., E. Tammpere, M. Kofoed, C. Keong, J. Chiang *et al.*, 2015 Complementation of yeast genes with human genes as an experimental platform for functional testing of human genetic variants. Genetics 201(3): 1263–1274.

Hanahan, D., and R. A. Weinberg, 2011 Hallmarks of cancer: the next generation. Cell 144(5): 646–674.

Hoffmann, W., 1985 Molecular characterization of the CAN1 locus in *Saccharomyces cerevisiae*. A transmembrane protein without N-terminal hydrophobic signal sequence. J. Biol. Chem. 260(21): 11831–11837.

Huang, M.-E., A.-G. Rio, A. Nicolas, and R. D. Kolodner, 2003 A genomewide screen in *Saccharomyces cerevisiae* for genes that suppress the accumulation of mutations. Proc. Natl. Acad. Sci. USA 100(20): 11529–11534.

Jackson, S. P., and J. Bartek, 2009 The DNA-damage response in human biology and disease. Nature 461(7267): 1071–1078.

Jain, S., N. Sugawara, A. Mehta, T. Ryu, and J. E. Haber, 2016 Sgs1 and Mph1 helicases enforce the recombination execution checkpoint during DNA double-strand break repair in *Saccharomyces cerevisiae*. Genetics 203(2): 667–675.

Johnson, R. E., 1999 Efficient bypass of a thymine-thymine dimer by yeast DNA polymerase, Pol. Science 283(5404): 1001–1004.

Kang, Y.-H., M.-J. Kang, J.-H. Kim, C.-H. Lee, I.-t. Cho *et al.*, 2009 The MPH1 gene of *Saccharomyces cerevisiae* functions in Okazaki fragment processing. J. Biol. Chem. 284(16): 10376–10386.

Kang, Y.-H., P. R. Munashingha, C.-H. Lee, T. A. Nguyen, and Y.-S. Seo, 2012 Biochemical studies of the *Saccharomyces cerevisiae* Mph1 helicase on junction-containing DNA structures. Nucleic Acids Res. 40(5): 2089–2106.

Kiiski, J. I., L. M. Pelttari, S. Khan, E. S. Freysteinsdottir, I. Reynisdottir *et al.*, 2014 Exome sequencing identifies FANCM as a susceptibility gene for triple-negative breast cancer. Proc. Natl. Acad. Sci. USA 111(42): 15172–15177.

Lang, G. I., and A. W. Murray, 2008 Estimating the per-base-pair mutation rate in the yeast *Saccharomyces cerevisiae*. Genetics 178(1): 67–82.

Lang, G. I., and A. W. Murray, 2011 Mutation rates across budding yeast chromosome VI are correlated with replication timing. Genome Biol. Evol. 3: 799–811.

Lisby, M., R. Rothstein, and U. H. Mortensen, 2001 Rad52 forms DNA repair and recombination centers during S phase. Proc. Natl. Acad. Sci. USA 98(15): 8276–8282.

Loeb, L. A., 2011 Human cancers express mutator phenotypes: origin, consequences and targeting. Nat. Rev. Cancer 11(6): 450–457.

Longtine, M. S., A. McKenzie, D. J. Demarini, N. G. Shah, A. Wach *et al.*, 1998 Additional modules for versatile and economical PCR-based gene deletion and modification in *Saccharomyces cerevisiae*. Yeast 14(10): 953–961.

Luke-Glaser, S., and B. Luke, 2012 The Mph1 helicase can promote telomere uncapping and premature senescence in budding yeast. PLoS One 7(7): e42028.

Luria, S. E., and M. Delbrück, 1943 Mutations of bacteria from virus sensitivity to virus resistance. Genetics 28(6): 491–511.

Mani, R., R. P. St.Onge, J. L. Hartman, G. Giaever, and F. P. Roth, 2008 Defining genetic interaction. Proc. Natl. Acad. Sci. USA 105(9): 3461–3466.

Mazón, G., and L. S. Symington, 2013 Mph1 and Mus81-Mms4 prevent aberrant processing of mitotic recombination intermediates. Mol. Cell 52(1): 63–74.

Mitchel, K., K. Lehner, and S. Jinks-Robertson, 2013 Heteroduplex DNA position defines the roles of the Sgs1, Srs2, and Mph1 helicases in promoting distinct recombination outcomes. *PLoS Genetics* 9(3): e1003340.

Negrini, S., V. G. Gorgoulis, and T. D. Halazonetis, 2010 Genomic instability–an evolving hallmark of cancer. Nat. Rev. Mol. Cell Biol. 11(3): 220–228.

Parenteau, J., and R. J. Wellinger, 1999 Accumulation of single-stranded DNA and destabilization of telomeric repeats in yeast mutant strains carrying a deletion of RAD27. Mol. Cell. Biol. 19(6): 4143–4152.

Peterlongo, P., J. Chang-Claude, K. B. Moysich, A. Rudolph, R. K. Schmutzler *et al.*, 2015 Candidate genetic modifiers for breast and ovarian cancer risk in BRCA1 and BRCA2 mutation carriers. Cancer Epidemiol. Biomarkers Prev. 24(1): 308–316.

Prakash, R., L. Krejci, S. Van Komen, K. Anke Schurer, W. Kramer *et al.*, 2005 *Saccharomyces cerevisiae* MPH1 gene, required for homologous recombination-mediated mutation avoidance, encodes a 3′ to 5′ DNA helicase. J. Biol. Chem. 280(9): 7854–7860.

Prakash, R., D. Satory, E. Dray, A. Papusha, J. Scheller *et al.*, 2009 Yeast Mph1 helicase dissociates Rad51-Made D-loops: implications for crossover control in mitotic recombination. Genes Dev. 23(1): 67–79.

Sanchez-Garcia, F., P. Villagrasa, J. Matsui, D. Kotliar, V. Castro *et al.*, 2014 Integration of genomic data enables selective discovery of breast cancer drivers. Cell 159(6): 1461–1475.

Scheller, J., A. Schürer, C. Rudolph, S. Hettwer, and W. Kramer, 2000 MPH1, a yeast gene encoding a DEAH protein, plays a role in protection of the genome from spontaneous and chemically induced damage. Genetics 155(3): 1069–1081.

Schurer, K. A., 2004 Yeast MPH1 gene functions in an error-free DNA damage bypass pathway that requires genes from homologous recombination, but not from postreplicative repair. Genetics 166(4): 1673–1686.

Shcherbakova, P. V., and T. A. Kunkel, 1999 Mutator phenotypes conferred by MLH1 overexpression and by heterozygosity for mlh1 mutations. Mol. Cell. Biol. 19(4): 3177–3183.

Stirling, P. C., M. S. Bloom, T. Solanki-Patil, S. Smith, P. Sipahimalani *et al.*, 2011 The complete spectrum of yeast chromosome instability genes identifies candidate CIN cancer genes and functional roles for ASTRA complex components. *PLoS Genetics* 7(4): e1002057.

Stirling, P. C., M. J. Crisp, M. A. Basrai, C. M. Tucker, M. J. Dunham *et al.*, 2012 Mutability and mutational spectrum of chromosome transmission fidelity genes. Chromosoma 121(3): 263–275.

Stirling, P. C., Y. Shen, R. Corbett, S. J. M. Jones, and P. Hieter, 2014 Genome destabilizing mutator alleles drive specific mutational trajectories in *Saccharomyces cerevisiae*. Genetics 196(2): 403–412.

Symington, L. S., 2002 Role of RAD52 epistasis group genes in homologous recombination and double-strand break repair. Microbiology and Molecular Biology Reviews: MMBR 66(4): 630–670.

Tishkoff, D. X., N. Filosi, G. M. Gaida, and R. D. Kolodner, 1997 A novel mutation avoidance mechanism dependent on *S. cerevisiae* RAD27 is distinct from DNA mismatch repair. Cell 88(2): 253–263.

Tong, A. H., M. Evangelista, A. B. Parsons, H. Xu, G. D. Bader *et al.*, 2001 Systematic genetic analysis with ordered arrays of yeast deletion mutants. Science 294(5550): 2364–2368.

Veitia, R. A., 2005 Gene dosage balance: deletions, duplications and dominance. Trends in Genetics: TIG 21(1): 33–35.

Vogelstein, B., and K. W. Kinzler, 2004 Cancer genes and the pathways they control. Nat. Med. 10(8): 789–799.

Winzeler, E. A., D. D. Shoemaker, A. Astromoff, H. Liang, K. Anderson *et al.*, 1999 Functional characterization of the *S. cerevisiae* genome by gene deletion and parallel analysis. Science 285(5429): 901–906.

Yuen, K. W. Y., C. D. Warren, O. Chen, T. Kwok, P. Hieter *et al.*, 2007 Systematic genome instability screens in yeast and their potential relevance to cancer. Proc. Natl. Acad. Sci. USA 104(10): 3925–3930.

Zack, T. I., S. E. Schumacher, S. L. Carter, A. D. Cherniack, G. Saksena *et al.*, 2013 Pan-cancer patterns of somatic copy number alteration. Nat. Genet. 45(10): 1134–1140.

Communicating editor: A. B. Britt

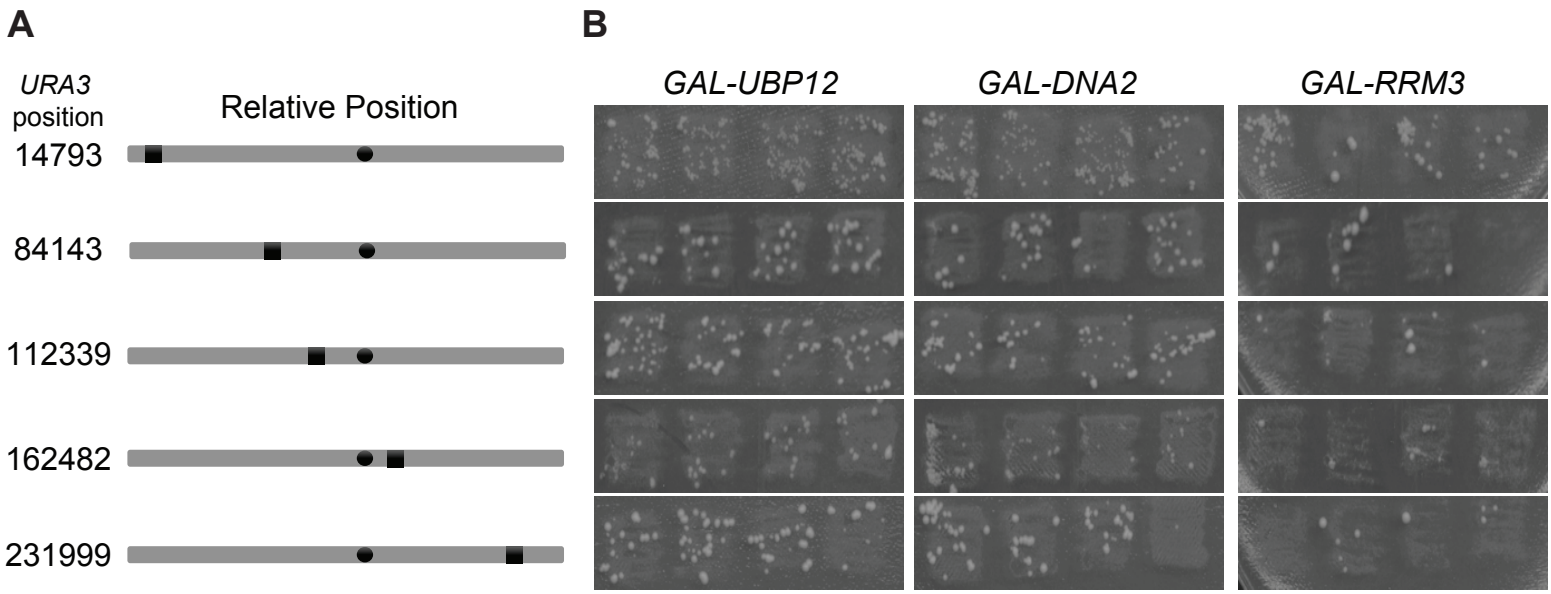

Figure S1. Positional effects of the dMutator phenotype. (A) Schematic of absolute and relative positions of *URA3* position along chromosome III. The black circle represents the centromere and the black boxes represent the location of the *URA3* gene relative to the centromere and the telomere. Numbers beside each schematic denotes the absolute position of *URA3* on the chromosome. (B) Strains containing *URA3* at positions indicated in A with a vector alone control or with the over-expression of *UBP12, DNA2* and *RRM3*. Each strain was assayed with four independent transformants.

Table S1: DNA helicases tested for dMutator phenotype. (.xlsx, 40 KB)

Available for download as a .xlsx file at:

http://www.genetics.org/lookup/suppl/doi:10.1534/genetics.116.192211/-/DC1/TableS1.xlsx

Table S2: Yeast strains and plasmids used in this study. (.xlsx, 38 KB)

Available for download as a .xlsx file at:

http://www.genetics.org/lookup/suppl/doi:10.1534/genetics.116.192211/-/DC1/TableS2.xlsx